Electronic Supplementary Material (ESI) for New Journal of Chemistry.

Supporting information

Construction of metal (Mn, Ce, Eu)-containing species in CN with photo-responsive oxidase-mimicking activity for antioxidants discrimination

Fan Du, Xiaojie Zhou, Yilian Bai, Qing Tang, Yunfei Cai* and Yurong Tang*

School of Chemistry and Chemical Engineering, Chongqing University, Chongqing 400044, China

*corresponding authors' E-mail: tangyuronga@cqu.edu.cn, yf.cai@cqu.edu.cn

Experimental Section

Materials and instruments

All reagents used in this work were analytical grade without further purification. Potassium Chloride(KCl), $MnCl_2.4H_2O$, $EuCl_3.6H_2O$, $CeCl_3.7H_2O$, hydrochloric acid (HCl), sodium hydroxide (NaOH) and Melamine ($C_3H_6N_6$) were brought from Kelong Reagent Company (Chengdu, China),ascorbic acid(AA), L-glutathione(GSH), Uric acid (UA), tannic acid (TCA), Dopamine (DA), L-cysteine(Cys) and Melatonin(MT) were purchased from Sangon Biotechnology Co. Ltd. (Shanghai,China). 3,3′,5,5′-tetramethylbenzidine (TMB), 2,2′-azino-bis(3-ethylbenzthiazoline-6-sulfonic acid) (ABTS) and o-phenylenediamine (OPD) were obtained from Aladin (Shanghai, China). All solutions were prepared using Milli-Q ultrapure water (18.2 MΩ).

Absorption measurements were performed on a TU-1901 spectrophotometer. X-ray diffraction (XRD) patterns were obtained on a Rigaku D/Max 2200PC diffractometer with Cu Kα radiation. Transmission electron microscopy (TEM) analyses were performed on a Philips Tecnai G2F20 microscope. X-ray photoelectron spectrometer(XPS) was operated on a Kratos XSAM800 spectrometer with a monochromatic Al Xray source (Al KR, 1.4866 keV). Fourier Transform Infrared (FTIR) spectra from 4000 to 400 cm^{-1} were recorded in KBr discs on a Nicolet IS10 FTIR spectrometer (Thermo Inc, America). Luminescence intensities were recorded using a RF-5301 RC. Photoluminescence spectras and lifetimes were recorded on an Edinburg Instruments FLS1000 spectrofluorometer at room temperature with a 450 W Xenon lamp and a 375 nm nanosecond Pulsed Diode laser (EPL), respectively.

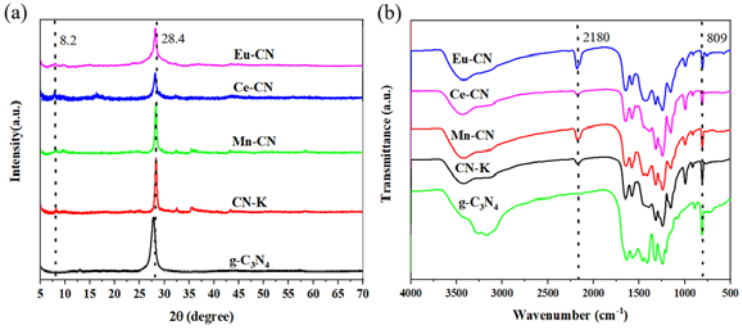

Figure S1. (a) XRD patterns and (b) FT-IR spectra of g-C_3N_4, CN-K, Mn-CN, Ce-CN and Eu-CN.

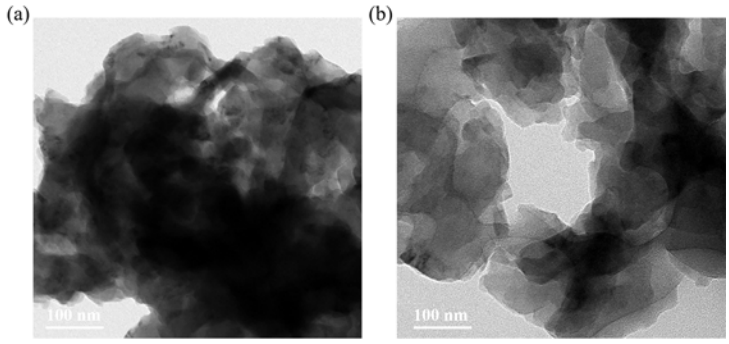

Figure S2. The TEM images of g-C_3N_4 (a), CN-K (b).

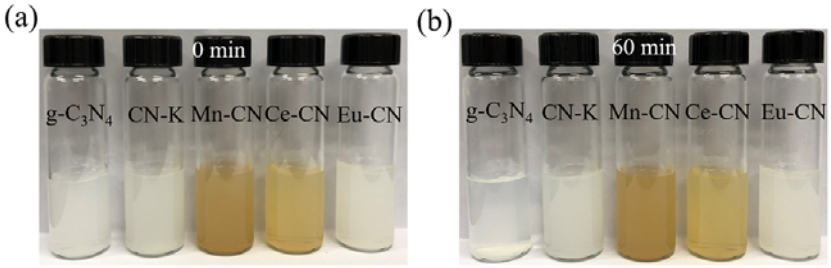

Figure S3. Suspension stability experiment. Pictures taken after different times: a) immediately after stop stirring; b) after 60 minutes.

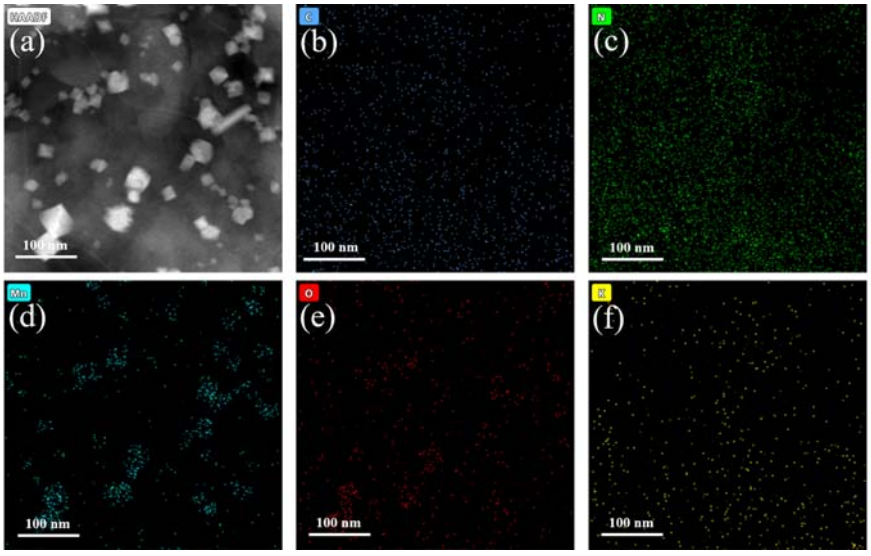

Figure S4. (a–f) HAADF-STEM elemental mapping images of the constituent elements in the Mn-CN catalyst.

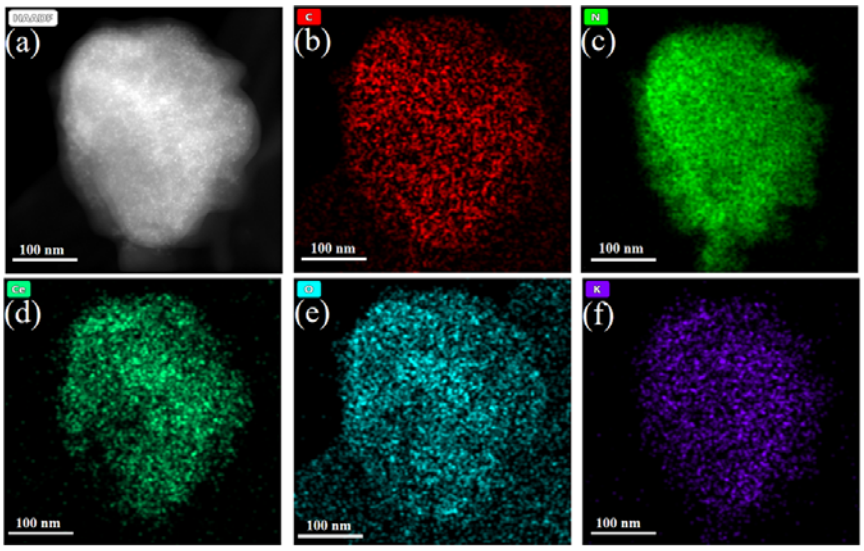

Figure S5. (a–f) HAADF-STEM elemental mapping images of the constituent elements in the Ce-CN catalyst.

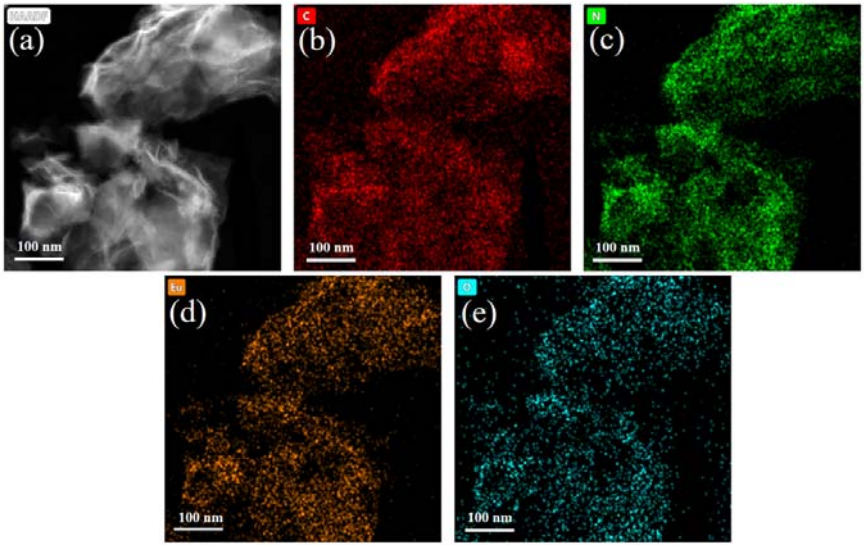

Figure S6. (a–e) HAADF-STEM elemental mapping images of the constituent elements in the Eu-CN catalyst.

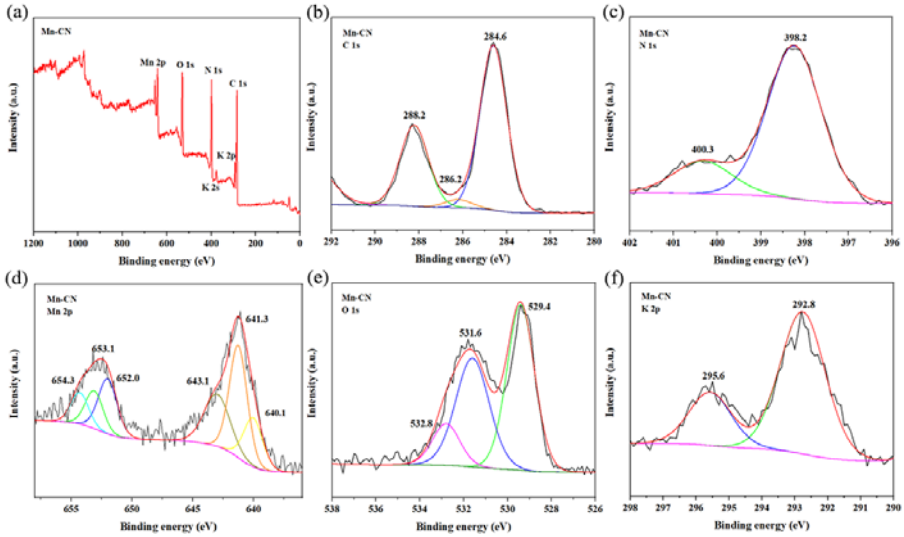

Figure S7. XPS spectrum of Mn-CN (a) survey spectra, (b) C 1s, (c) N 1s, (d) Mn 2p, (e) O 1s, (f) K 2p high-resolution spectra.

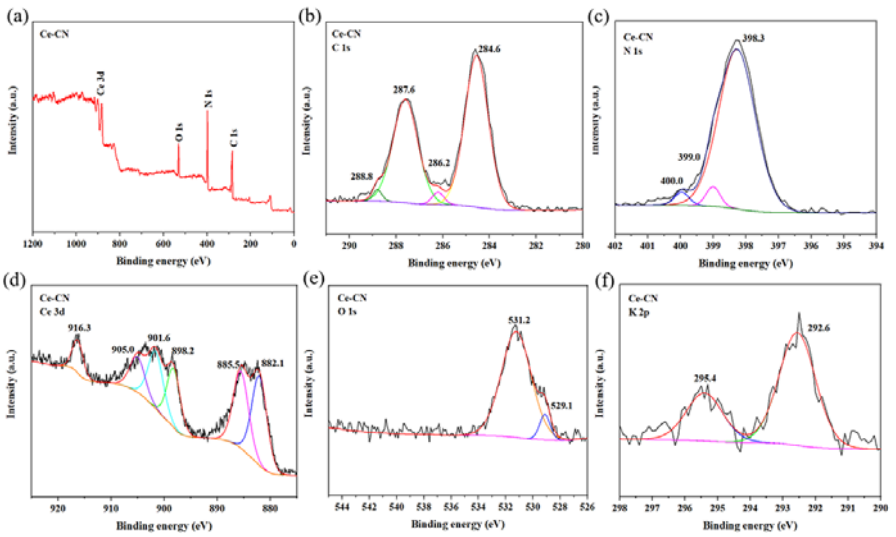

Figure S8. XPS spectrum of Ce-CN (a) survey spectra, (b) C 1s, (c) N 1s, (d) Ce 3d, (e) O 1s, (f) K 2p high-resolution spectra.

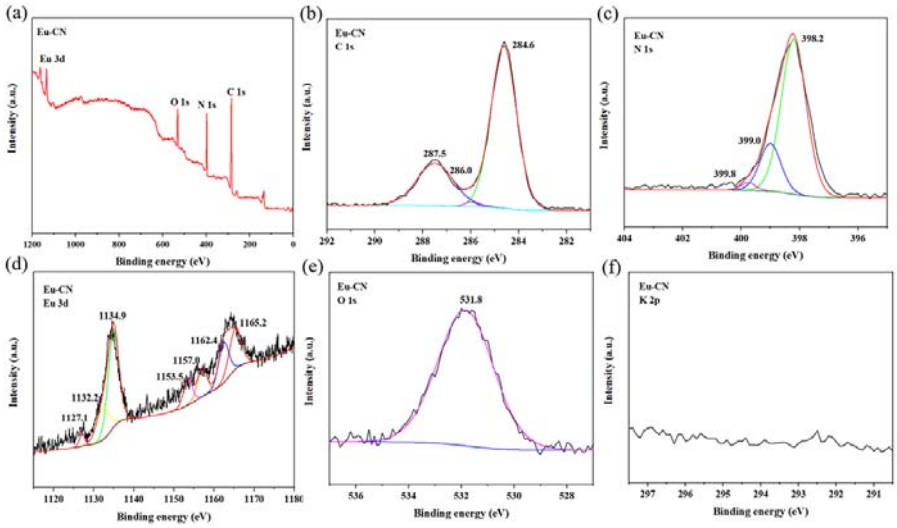

Figure S9. XPS spectrum of Eu-CN (a) survey spectra, (b) C 1s, (c) N 1s, (d) Eu 3d, (e) O 1s, (f) K 2p high-resolution spectra.

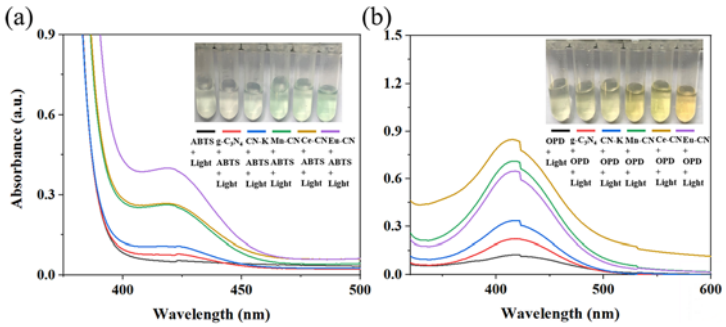

Figure S10. The UV–vis absorption curves of different reaction systems used (a) ABTS and (b) OPD as substrates.

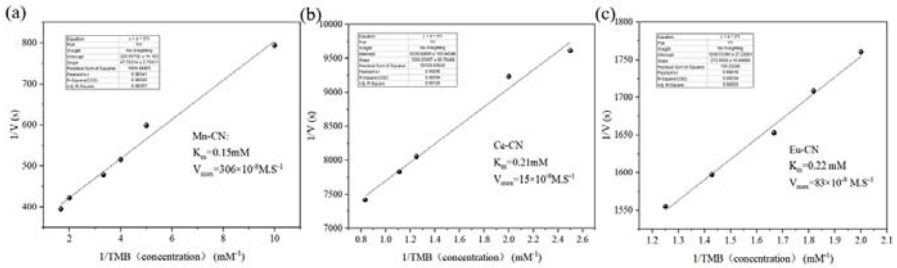

Figure S11. Steady-state kinetic analysis of (a) Mn-CN, (b) Ce-CN and (c) Eu-CN as photo-oxidase mimics to TMB. The velocity (v) of the reaction was measured using 30 $\mu g \cdot mL^{-1}$ catalyst.

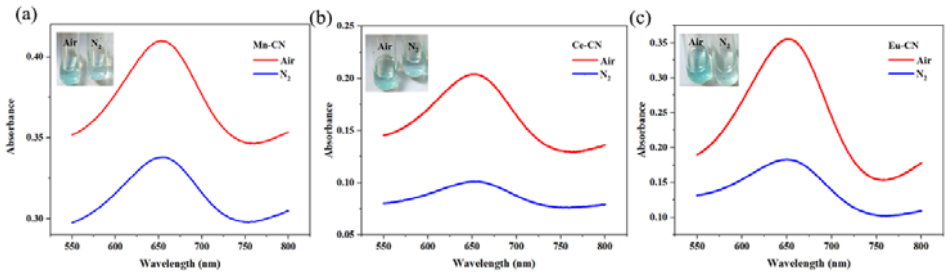

Figure S12. Effect of atmosphere for (a) Mn-CN, (b) Ce-CN and (c) Eu-CN catalyze oxidation coloration. Inset is the corresponding photograph.

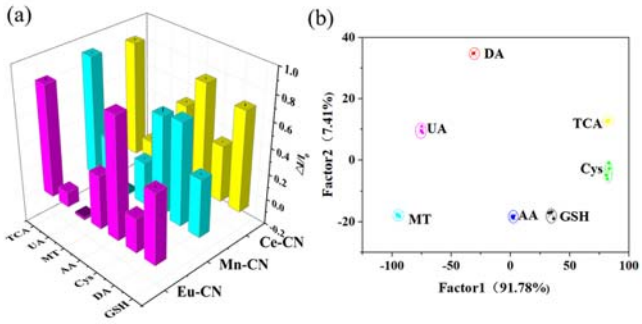

Figure S13. Fingerprints for seven antioxidants (3 μM) generated from photocolorimetric response patterns. b) Canonical score plot for the triple-channel signal patterns obtained from LDA against seven antioxidants (3 μM).

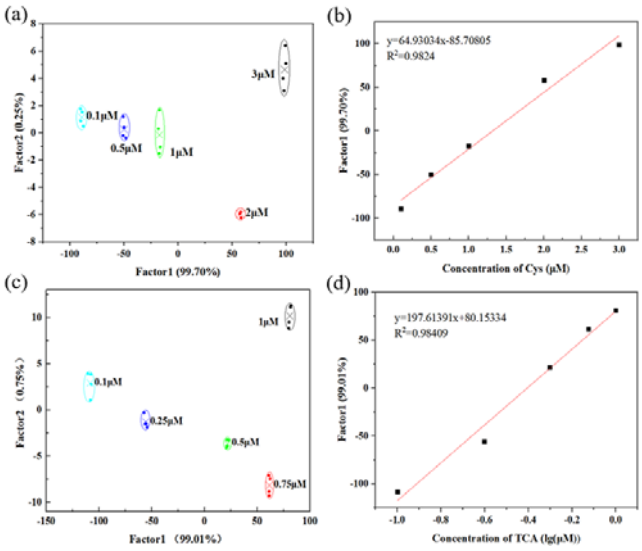

Figure S14. LDA plots for (a) Cys at different concentrations (0.1, 0.5, 1, 2 and 3 μM), and (b) Plot of the discriminant factor 1 versus the Cys concentration. (c) TCA at various concentrations (0.1, 0.25, 0.5, 0.75 and 1 μM) and (d) Plot of the discriminant factor 1 versus the logarithm of TCA concentration.

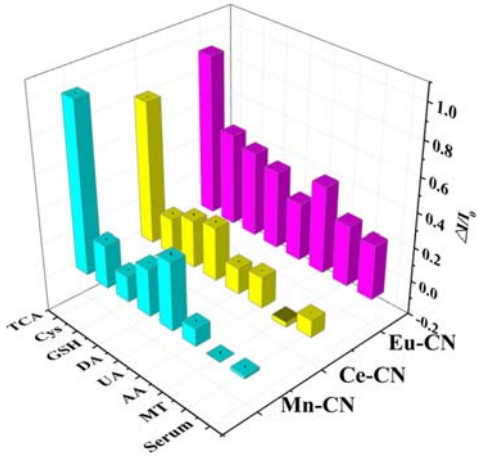

Figure S15. Fingerprints for seven antioxidants (1 μM) spiked in the human serum.

Table S1. Surface atomic ratios of all elements measured by XPS

Sample	Atomic content （%）					C/N
	C	N	O	K	M	
Mn-CN	26.96%	37.98%	25.05%	3.96%	6.05%	0.71
Ce-CN	34.17%	43.82%	17%	1.78%	3.2%	0.78
Eu-CN	36.2%	50.6%	10.38%	/	2.79%	0.71

Table S2. Comparison of K_m and V_{max} of Mn-CN, Eu-CN, Ce-CN and the reported nanomaterials with oxidase-like activity.

Catalyst	Substrate	K_m/mM	$V_{max}/10^{-8}$ M.s^{-1}	Reference
HPR	TMB	4.3×10^{-1}	10	[S1]
MSN-Au NPs	TMB	2.25×10^{-1}	12	[S2]
WS_2	TMB	1.83	4.31	[S3]
Au/CeO_2 CSNPs	TMB	2.9×10^{-1}	3.9	[S4]
Porous g-C3N4	TMB	5.8×10^{-1}	5.84	[S5]
GO-Fe_3O_4 NPs	TMB	4.3×10^{-1}	13.8	[S6]
$ZnFe_2O_4$	TMB	0.85	13.31	[S7]
Mn-CN	TMB	1.5×10^{-1}	306	This work
Ce-CN	TMB	2.1×10^{-1}	15	This work
Eu-CN	TMB	2.2×10^{-1}	83	This work

Table S3. The training matrix of the colorimetric response patterns against 7 antioxidants using this sensor assay at the concentration of 1μM.

antioxidants	I_0-I/I_0 Eu-CN	I_0-I/I_0 Mn-CN	I_0-I/I_0 Ce-CN
GSH	0.326769	0.165796	0.223489
GSH	0.332429	0.169152	0.242142
GSH	0.34009	0.1624	0.258722
GSH	0.356476	0.160847	0.203454
DA	0.15142	0.297906	0.190095

DA	0.1461	0.290234	0.152716
DA	0.13807	0.295248	0.198843
DA	0.14885	0.290633	0.193493
TCA	0.868404	0.949537	0.820433
TCA	0.90073	0.948957	0.849214
TCA	0.888464	0.948912	0.862018
TCA	0.91162	0.955649	0.837469
Cys	0.309773	0.280073	0.404539
Cys	0.304993	0.298709	0.364619
Cys	0.31002	0.292742	0.360345
Cys	0.298709	0.302522	0.395845
AA	0.285869	0.19782	0.390171
AA	0.266825	0.194	0.389114
AA	0.302915	0.19947	0.395949
AA	0.278345	0.20093	0.398274
MT	0.002462	0.090432	0.083266
MT	-0.0221	0.075818	0.091784
MT	-0.03847	0.098965	0.089434
MT	-0.06763	0.070521	0.078934
UA	-0.0146	0.309713	0.07563
UA	-0.01857	0.298398	0.069462
UA	-0.03476	0.298709	0.051766
UA	-0.04737	0.330035	0.054336

Table S4. The training matrix of the colorimetric response patterns against 7 antioxidants using this sensor assay at the concentration of 3μM.

antioxidants	**I_0-I/I_0 Eu-CN**	**I_0-I/I_0 Mn-CN**	**I_0-I/I_0 Ce-CN**
GSH	0.541386	0.446543	0.756927
GSH	0.538172	0.442377	0.754686
GSH	0.521068	0.434044	0.754252
GSH	0.530655	0.428973	0.783317
DA	0.257579	0.765159	0.424113
DA	0.257633	0.767921	0.429474
DA	0.258014	0.767876	0.430722
DA	0.266294	0.769144	0.422425
Cys	0.907624	0.768235	0.830469
Cys	0.903198	0.753452	0.837424
Cys	0.901947	0.722747	0.819094
Cys	0.904064	0.713331	0.824745
AA	0.394305	0.319307	0.597237
AA	0.409735	0.323267	0.593782
AA	0.405065	0.313366	0.593092

AA	0.404862	0.314356	0.582729
MT	-0.00695	-0.00865	0.118364
MT	-0.02116	-0.01223	0.113371
MT	-0.02329	-0.00815	0.108892
MT	-0.02291	-0.00471	0.125927
UA	0.119161	0.345786	0.15963
UA	0.114749	0.343477	0.171672
UA	0.11306	0.346602	0.161686
UA	0.111698	0.363402	0.168588
TCA	0.834309	0.90945	0.891333
TCA	0.836066	0.914195	0.892
TCA	0.864754	0.920127	0.874
TCA	0.86534	0.914986	0.873333

Table S5. Identification of blind samples with 1μM antioxidants.

Samples	Eu-CN	Mn-CN	Ce-CN	Identification	Verification
1	0.287745	0.196253	0.394521	AA	AA
2	-0.045261	0.087426	0.077314	MT	MT
3	0.305743	0.297803	0.367415	Cys	Cys
4	0.149971	0.295246	0.200121	DA	DA
5	0.327964	0.165742	0.239471	GSH	GSH
6	0.896641	0.948963	0.838049	TCA	TCA
7	-0.023196	0.327461	0.061594	UA	UA
8	0.340053	0.168916	0.240573	GSH	GSH
9	0.341279	0.162544	0.251126	GSH	GSH
10	-0.032792	0.330124	0.058699	UA	UA
11	0.900021	0.952347	0.845911	TCA	TCA
12	0.141573	0.291733	0.197523	DA	DA
13	0.302911	0.286411	0.375273	Cys	Cys
14	-0.051523	0.073229	0.079428	MT	MT
15	0.279562	0.195791	0.394733	AA	AA
16	0.879643	0.954159	0.861672	TCA	TCA
17	0.152475	0.294223	0.198814	DA	DA
18	0.299752	0.301724	0.396691	Cys	Cys
19	0.001321	0.095231	0.090377	MT	MT
20	0.294673	0.281252	0.392547	AA	Cys
21	-0.019971	0.298563	0.057323	UA	UA
22	0.333097	0.164756	0.236782	GSH	GSH
23	-0.031246	0.307942	0.053496	UA	UA
24	0.884124	0.947612	0.857914	TCA	TCA
25	0.285673	0.196625	0.399122	AA	AA
26	0.002154	0.072688	0.088697	MT	MT
27	0.137982	0.300107	0.195739	DA	DA

28	0.297436	0.200751	0.389002	AA	AA

Table S6. The training matrix of the colorimetric response patterns against Cys at different concentration using this sensor assay.

antioxidants	I_0-I/I_0 Eu-CN	I_0-I/I_0 Mn-CN	I_0-I/I_0 Ce-CN
Cys 5μM	0.969016	0.984943	0.912554
Cys 5μM	0.955833	0.985944	0.903425
Cys 5μM	0.954582	0.983761	0.906106
Cys 5μM	0.967284	0.985171	0.928899
Cys 3μM	0.907624	0.768235	0.830469
Cys 3μM	0.903198	0.753451	0.837424
Cys 3μM	0.901947	0.722747	0.819094
Cys 3μM	0.904064	0.71333	0.824745
Cys 1μM	0.24076	0.292742	0.404539
Cys 1μM	0.280073	0.284008	0.364619
Cys 1μM	0.298709	0.302522	0.360345
Cys 1μM	0.243466	0.279096	0.395845
Cys 0.5μM	0.174584	0.14777	0.208708
Cys 0.5μM	0.149565	0.168649	0.206245
Cys 0.5μM	0.153607	0.145177	0.20319
Cys 0.5μM	0.184014	0.145632	0.190082
Cys 0.1μM	0.007538	0.009712	0.023809
Cys 0.1μM	-0.01806	0.013169	0.022776
Cys 0.1μM	-0.01738	0.025087	0.02092
Cys 0.1μM	0.004747	0.020038	0.017515

Table S7. The training matrix of the colorimetric response patterns against TCA at different concentration using this sensor assay.

antioxidants	I_0-I/I_0 Eu-CN	I_0-I/I_0 Mn-CN	I_0-I/I_0 Ce-CN
TCA 5μM	0.977752	0.965758	0.954741
TCA 5μM	0.97786	0.977668	0.972322
TCA 5μM	0.976136	0.981876	0.974646
TCA 5μM	0.978614	0.969448	0.963604
TCA 1μM	0.752902	0.877683	0.875774
TCA 1μM	0.781507	0.883707	0.872868
TCA 1μM	0.778867	0.894363	0.87236
TCA 1μM	0.745684	0.8939	0.87127
TCA 0.5μM	0.387238	0.814672	0.642578
TCA 0.5μM	0.374579	0.812355	0.654783
TCA 0.5μM	0.378242	0.815135	0.652386
TCA 0.5μM	0.390955	0.816988	0.653984
TCA 0.25μM	0.118	0.490811	0.333684

TCA 0.25μM	0.114553	0.51861	0.334919
TCA 0.25μM	0.113314	0.509344	0.33521
TCA 0.25μM	0.111051	0.506564	0.333975
TCA 0.1μM	-0.04743	0.238301	0.156063
TCA 0.1μM	-0.0449	0.233205	0.194057
TCA 0.1μM	-0.07614	0.254054	0.187519
TCA 0.1μM	-0.04926	0.255907	0.172191

Table S8. Training matrix of response patterns against Cys、AA、TCA at different concentration

antioxidants	I_0-I/I_0 Eu-CN	I_0-I/I_0 Mn-CN	I_0-I/I_0 Ce-CN
TCA 5μM	0.977752	0.965758	0.954741
TCA 5μM	0.97786	0.977668	0.972322
TCA 5μM	0.976136	0.981876	0.974646
TCA 5μM	0.978614	0.969448	0.963604
TCA 1μM	0.752902	0.877683	0.875774
TCA 1μM	0.781507	0.883707	0.872868
TCA 1μM	0.778867	0.894363	0.87236
TCA 1μM	0.745684	0.8939	0.87127
TCA 0.5μM	0.387238	0.814672	0.642578
TCA 0.5μM	0.374579	0.812355	0.654783
TCA 0.5μM	0.378242	0.815135	0.652386
TCA 0.5μM	0.390955	0.816988	0.653984
Cys 5μM	0.969016	0.984943	0.912554
Cys 5μM	0.955833	0.985944	0.903425
Cys 5μM	0.954582	0.983761	0.906106
Cys 5μM	0.967284	0.985171	0.928899
Cys 1μM	0.24076	0.292742	0.404539
Cys 1μM	0.280073	0.284008	0.364619
Cys 1μM	0.298709	0.302522	0.360345
Cys 1μM	0.243466	0.279096	0.395845
Cys 0.5μM	0.174584	0.14777	0.208708
Cys 0.5μM	0.149565	0.168649	0.206245
Cys 0.5μM	0.153607	0.145177	0.20319
Cys 0.5μM	0.184014	0.145632	0.190082
AA 5μM	0.772928	0.712779	0.73886
AA 5μM	0.717556	0.707516	0.760967
AA 5μM	0.759478	0.709128	0.75544
AA 5μM	0.757245	0.712542	0.760276
AA 1μM	0.126024	0.139	0.390171
AA 1μM	0.128711	0.137293	0.389114
AA 1μM	0.123788	0.143646	0.395949
AA 1μM	0.122925	0.146681	0.398274

AA 0.5μM	0.053444	0.098652	0.276731
AA 0.5μM	0.042481	0.0877	0.276026
AA 0.5μM	0.05182	0.090497	0.289625
AA 0.5μM	0.052276	0.066934	0.286947

Table S9. The training matrix of the colorimetric response patterns against the mixture of TCA and UA at 0.75 μM using this sensor assay.

antioxidants	I_0-I/I_0 Eu-CN	I_0-I/I_0 Mn-CN	I_0-I/I_0 Ce-CN
TCA	0.60518	0.971154	0.824738
TCA	0.586553	0.972754	0.825078
TCA	0.583246	0.972604	0.819172
TCA	0.590962	0.976203	0.819104
TCA/UA 75:25	0.523009	0.969704	0.719323
TCA/UA 75:25	0.517994	0.970904	0.722038
TCA/UA 75:25	0.503004	0.973354	0.725364
TCA/UA 75:25	0.50124	0.971704	0.706698
TCA/UA 50:50	0.291099	0.846921	0.612483
TCA/UA 50:50	0.289722	0.849621	0.610243
TCA/UA 50:50	0.28895	0.845621	0.613501
TCA/UA 50:50	0.285699	0.849871	0.62314
TCA/UA 25:75	0.115955	0.676195	0.294948
TCA/UA 25:75	0.107964	0.675445	0.31375
TCA/UA 25:75	0.110554	0.657147	0.306216
TCA/UA 25:75	0.106751	0.654198	0.302075
UA	0.003582	0.371886	-0.0699
UA	0.021163	0.364337	-0.04757
UA	0.010251	0.365987	-0.05327
UA	0.022706	0.368987	-0.06189

Table S10. The training matrix of the colorimetric response patterns against the antioxidants at 1 μM in serum samples using this sensor assay.

antioxidants	I_0-I/I_0 Eu-CN	I_0-I/I_0 Mn-CN	I_0-I/I_0 Ce-CN
GSH	0.490201	0.152234	0.260061
GSH	0.492018	0.145119	0.277948
GSH	0.490006	0.147259	0.274371
GSH	0.483452	0.143033	0.270857
DA	0.451463	0.271713	0.292349
DA	0.443344	0.268812	0.305581
DA	0.441556	0.269984	0.308136
DA	0.442322	0.267251	0.304664
Cys	0.535260	0.256285	0.212694
Cys	0.530306	0.242644	0.210860
Cys	0.531430	0.244249	0.202869

Cys	0.527600	0.248207	0.201034
MT	0.348465	-0.016869	-0.029346
MT	0.346422	0.008809	-0.029673
MT	0.348363	0.007632	-0.025874
MT	0.343154	0.007204	-0.033407
TCA	0.933615	0.982773	0.817426
TCA	0.930449	0.990745	0.817299
TCA	0.929479	0.989728	0.819087
TCA	0.930705	0.983362	0.820620
UA	0.329850	0.373016	0.145074
UA	0.328358	0.403937	0.145138
UA	0.327839	0.405488	0.152996
UA	0.327449	0.382217	0.153634
AA	0.499351	0.100407	0.175546
AA	0.494419	0.088581	0.179506
AA	0.493380	0.106096	0.177398
AA	0.500778	0.101969	0.174715
Serum	0.316294	0.017403	0.097994
Serum	0.313537	0.026496	0.096141
Serum	0.309094	0.014559	0.097930
Serum	0.307205	0.012327	0.099910

Table S11. The training matrix of the colorimetric response patterns against antioxidant mixtures at 1 μM in serum samples using this sensor assay.

antioxidants	**I_0-I/I_0 Eu-CN**	**I_0-I/I_0 Mn-CN**	**I_0-I/I_0 Ce-CN**
Serum	0.25726919	0.031759	0.138017739
Serum	0.31044829	0.013463	0.135842652
Serum	0.24430012	0.022496	0.137138448
Serum	0.26897037	-0.00162	0.134778248
GSH	0.50652401	0.279199	0.256305437
GSH	0.49710811	0.35046	0.253251059
GSH	0.49456168	0.273585	0.253112224
GSH	0.45518072	0.273897	0.256814499
UA	0.32768116	0.295182	0.12344003
UA	0.30162459	0.297287	0.125855764
UA	0.27698928	0.30828	0.123069802
UA	0.27651552	0.297287	0.109047434
TCA	0.80291755	0.930376	0.810212109
TCA	0.79421228	0.92905	0.801141535
TCA	0.79622574	0.926166	0.801419205
TCA	0.7966995	0.92944	0.796745083
TCA+UA	0.41603664	0.908311	0.53661396
TCA+UA	0.42346151	0.903945	0.541149247

TCA+UA	0.447362	0.929674	0.526293867
TCA+UA	0.43386717	0.923281	0.549757037
TCA+GSH	0.58707964	0.939498	0.609548785
TCA+GSH	0.57672818	0.927803	0.618526802
TCA+GSH	0.56675609	0.932949	0.619128422
TCA+GSH	0.56204103	0.9356	0.603208638
UA+GSH	0.40048235	0.496647	0.189849594
UA+GSH	0.37674444	0.495946	0.198688776
UA+GSH	0.38877598	0.493685	0.20391824
UA+GSH	0.37132482	0.493919	0.200725028
UA+TCA+GSH	0.52280302	0.914549	0.465715387
UA+TCA+GSH	0.52811425	0.918447	0.462290782
UA+TCA+GSH	0.53369645	0.919149	0.442900115
UA+TCA+GSH	0.533750644	0.922579136	0.447296567

Supporting references

[S1] Gao LZ, Zhuang J, Nie L, Zhang JB, Zhang Y, Gu N, Wang TH, Feng J, Yang DL, Perrett S, Yan XY (2007) Intrinsic peroxidase-like activity of ferromagnetic nanoparticles. Nat Nanotechnol 2: 577–583

[S2] Tao Y, Lin YH, Huang ZZ, Ren JS, Qu XG (2013) Incorporating graphene oxide and gold nanoclusters: a synergistic catalyst with surprisingly high peroxidase-like activity over a broad pH range and its application for cancer cell detection. Adv Mater 25: 2594–2599

[S3] Lin TR, Zhong LS, Song ZP, Guo LQ, Wu HY, Guo QQ, Chen Y, Fu FF, Chen GN (2014) Visual detection of blood glucose based on peroxidase-like activity of WS_2 nanosheets. Biosens Bioelectron 62: 302–307

[S4] Bhagat S, Srikanth Vallabani N, Shutthanandan V, Bowden M, Karakoti AS, Singh S (2018) Gold core/ceria shell-based redox active nanozyme mimicking the biological multienzyme complex phenomenon. J Colloid Interface Sci 513: 831–842

[S5] Wang Y, Liu RL, Chen GN, Wang L, Yu P, Shu H, Bashir K, Fu Q (2019) Hemin-porous g-C_3N_4 hybrid nanosheets as an efficient peroxidase mimic for colorimetric and visual determination of glucose. Microchim Acta 186: 446

[S6] Dong YL, Zhang HG, Rahman ZU, Su L, Chen XJ, Hu J, Chen XJ (2012) Graphene oxide-Fe_3O_4 magnetic nanocomposites with peroxidase-like activity for colorimetric detection of glucose. Nanoscale 4: 3969–3976

[S7] Su L, Feng J, Zhou XM, Ren CL, Li HH, Chen XG (2012) Colorimetric detection of urine glucose based $ZnFe_2O_4$ magnetic nanoparticles. Anal Chem 84: 5753−5758